Discovery of novel antibiotics from actinomycetes by integrated metabolomics & genomics approaches

Wu, Changsheng

Chapter 8

Lugdunomycin, a novel angucycline derivative with unprecedented chemical architecture

Changsheng Wu [1,2], Helga van der Heul [1], Young Hae Choi [2], and Gilles P. van Wezel [1]

[1] *Molecular Biotechnology, Institute of Biology, Leiden University, Sylviusweg 72, 2333 BE, The Netherlands*
[2] *Natural Products Laboratory, Institute of Biology, Leiden University, Sylviusweg 72, 2333 BE, The Netherlands*

Manuscript in preparation
Patent application PCT/NL2016/050398

ABSTRACT

The discovery of new lead compounds from natural sources is pivotal to replenish the drug discovery pipelines. Here we describe lugdunomycin (**1**), a novel angucycline polyketide bearing unprecedented chemical skeleton produced by *Streptomyces* species QL37. Lugdunomycin shows unique structural characteristics: a heptacyclic 6/6/5/6/6/5/5 ring system, a spiroatom, two all-carbon stereogenic centers, and a benzaza[4,3,3]propellane motif. Detailed metabolic analysis of the producer strain allowed the characterization of in total 31 angucyclines, whereby **5**–**7**, **10**, **11**, **16**–**21**, **24**, **26**–**31** were new compounds. The derivatization mechanisms of the characterized angucyclines **2**–**31** provided insights to understand the structural complexity in biosynthesis pathway of lugdunomycin (**1**), which involves both enzymatic catalysis and nonenzymatic chemistry, including Baeyer-Villiger oxidative cleavage, amidation, Diels–Alder reaction, intermolecular Michael addition, and nucleophilic Favorskii rearrangement. Metabolite-guided genome mining of *Streptomyces* sp. QL37 combined with genetic disruption identified a type II PKS gene cluster (*lug*) responsible for biosynthesis of compounds **1**–**31**, among which, *lugOII* was the gene encoding the key oxygenase responsible for the Baeyer-Villiger oxidative cleavage of quinone in angucycline backbone.

1. INTRODUCTION

While the twentieth century witnessed the dramatic successes of antimicrobial agents delivered by the pharmaceutical industry, with an explosive growth in the golden era during 1940s to 1960s, the introduction of major new classes of natural product-based antibacterial agents has now come to a near standstill.[1] The approval of the last antibiotic daptomycin in 2003 marked the launch of the first natural product-based antibiotic in decades.[2,3] The continuous emergence of "untreatable superbugs" threatens to outpace the discovery of new anti-infectives. It is therefore imperative that novel antimicrobials are developed to reverse this negative trend.[4]

Actinomycetes are industrially and medicinally important microorganisms for their ability to produce a plethora of secondary metabolites. More than two-thirds of the known antibiotics are produced by this type of filamentous bacteria, with *Streptomyces* as the major producers.[5] The advent of next-generation sequencing (NGS) technologies has uncovered that even the best-studied model actinomycete *Streptomyces coelicolor* A(3)2 still possesses many yet underexplored resources for natural products.[6] As the increasing number of sequenced genomes of actinomycetes reveal a plethora of novel biosynthetic genes, natural product drug discovery is entering an exciting second golden age.[7] Efforts are therefore required to exploit this huge unexplored reservoir of bioactive natural products.[8]

Angucyclines and angucyclinones bearing an unsymmetrically assembled benz[a]anthracene frame represents the largest family of polycyclic aromatic polyketides from actinomycetes, and exhibit a broad range of biological activities, predominantly anticancer and antibacteria. All angucycline/ones are biosynthesized by type II polyketide synthases (PKSs), via aldol decarboxylative condensations of an acyl-CoA starter and nine malonyl-CoA extenders, to form the initial framework that could be further modified by a wide array of post-PKS tailoring enzymes. The vast structural diversity of angucycline group antibiotics could partially arise from functionality variations, such as hydroxylation, epoxidation, glycosylation at various positions, while the basic angular tetracyclic backbone remains intact. More intriguingly, the referred scaffold could be drastically modified through oxidative ring-cleavages, followed by rearrangement reactions or incorporations of additional carbon units to form new ring(s) system.[9,10] Therefore, angucycline-based polyketides are a rich family of chemical structures with many different features and bioactivities.

Herein, we report the isolation, structure elucidation, and antimicrobial property of a novel angucycline-derived compound, lugdunomycin (**1**) with striking backbone of benzaza[4,3,3]propellane-6-spiro-2'-2*H*-naphtho[1,8-*bc*]furan, from a soil-derived *Streptomyces* sp. QL37. Application of the OSMAC (one strain many compounds) strategy to this strain allowed the characterization of 30 other rearranged and/or unrearranged angucyclines **2—31**, whereby 18 compounds were new structures featuring unique ring rearrangement, oxidation, and amidation. The structural relationship among compounds **2—31** shed light on the convergent biosynthesis of lugdunomycin (**1**) through a Diels–Alder reaction. Metabolite-guided genome mining of *Streptomyces* sp. QL37 in combination with molecular biology approaches identified a type II PKS gene cluster (*lug*) responsible for the biosynthesis of the characterized angucycline/ones. The new structural features described in this study, especially the C-ring cleavage and expansion, enrich the existent diversity of the angucycline/one type natural products, while the biosynthetic logic for lugdunomycin (**1**)

could be potentially exploited to add chemical diversity and/or pharmaceutical significance to other polyketide skeletons (such as tetracycline antibiotics), either through biochemical or synthetic approaches.

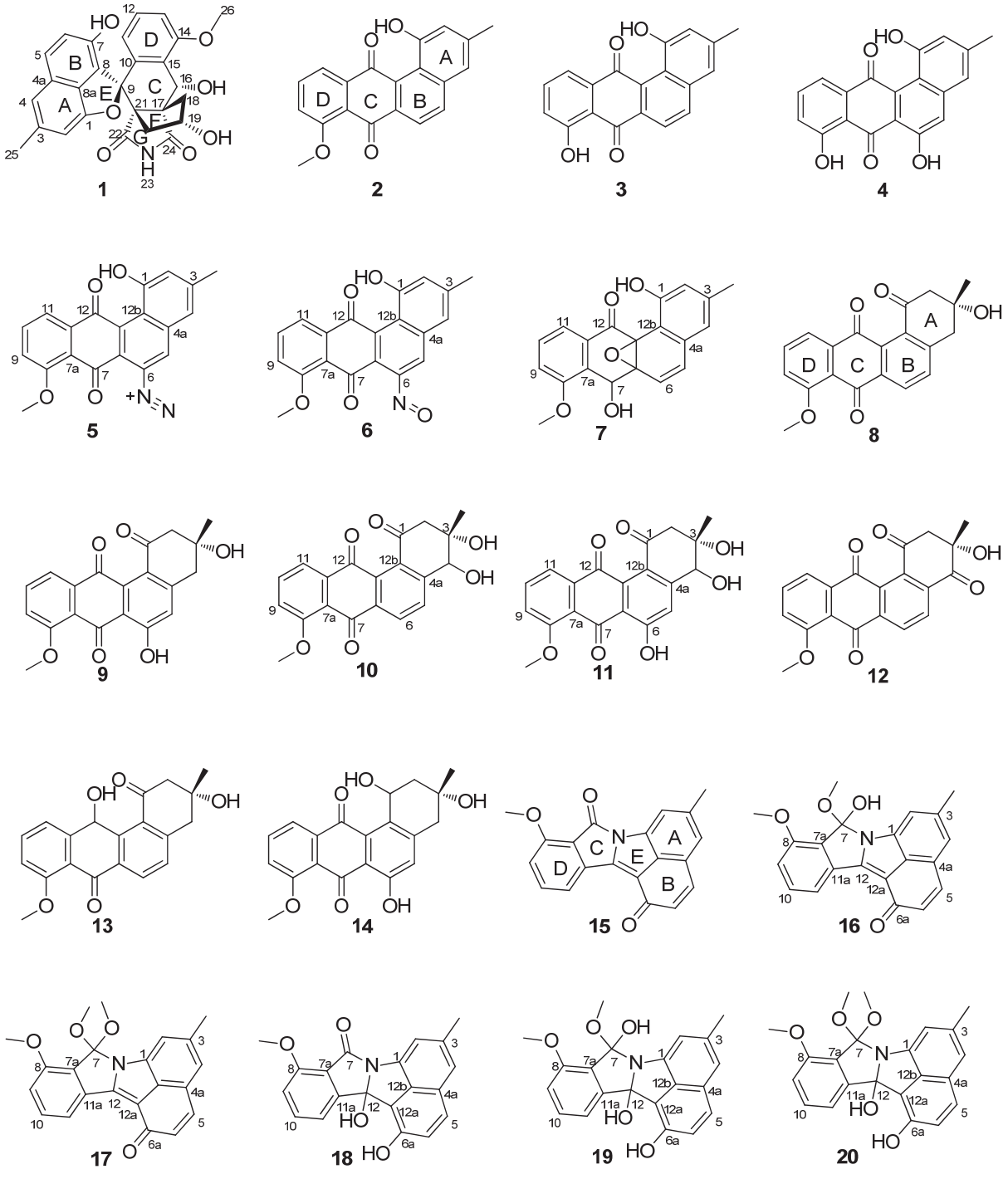

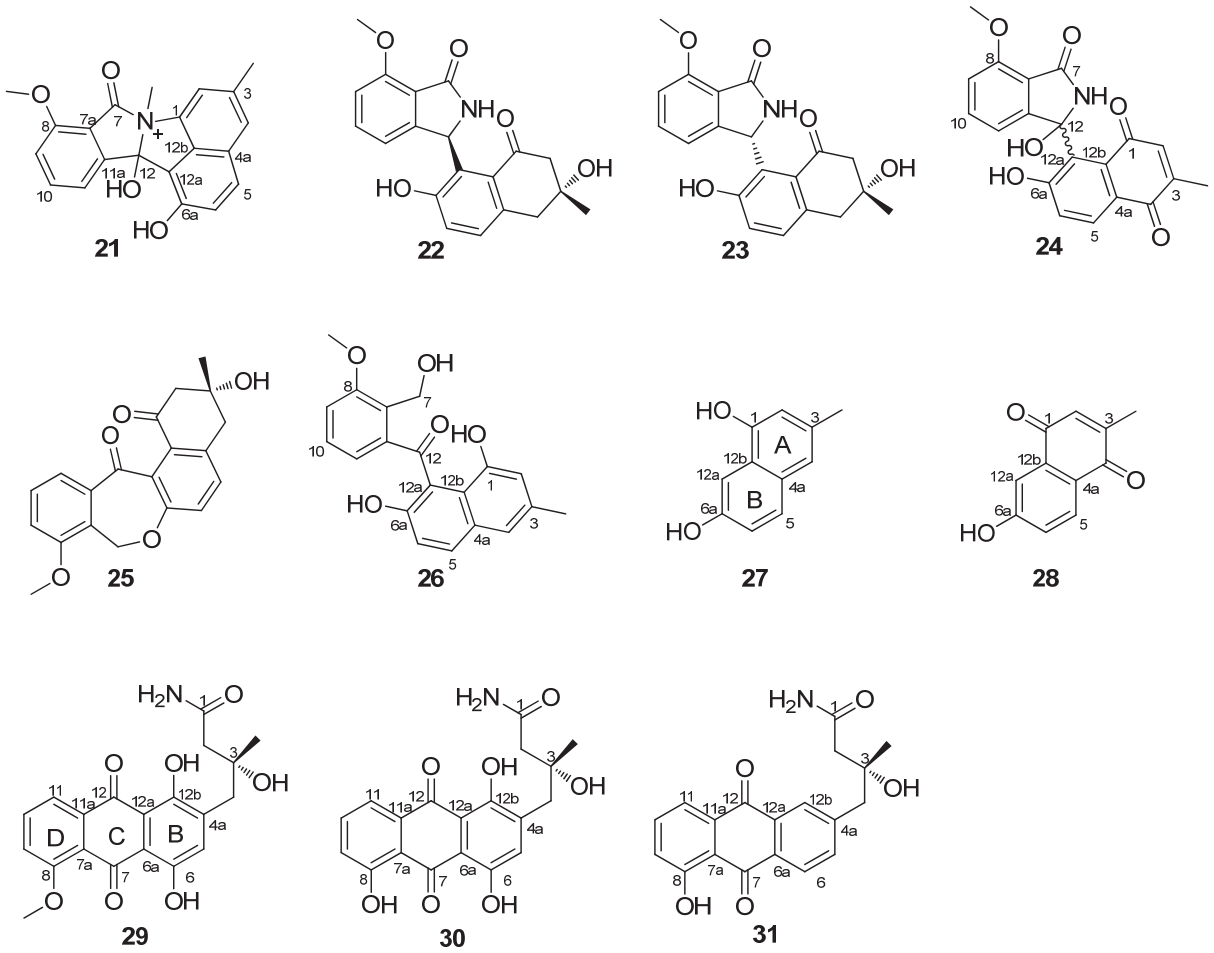

Figure 1. Rearranged and unrearranged angucyclines from *Streptomyces sp*. QL37. Lugdunomycin (**1**) is a novel angucycline derivative with unprecedented skeleton. All compounds are biosynthetically related (see Figure 3), whereby **5—7**, **10**, **11**, **16—21**, **24**, **26—31** with carbon numbering, are novel compounds.

2. RESULTS AND DISCUSSION

2.1. Discovery of lugdunomycin (1)

In our search for novel antibiotics, seven strains showing distinctive pigmentation were prioritized out of a unique collection of 816 actinomycetes,[11] because the presence of distinctive color is a marker for secondary metabolite biosynthesis.[12] The metabolic profile of a given actinomycete is culture media-dependent, and varying growth conditions or the addition of chemical elicitors can often be applied to activate the biosynthesis of poorly expressed natural products.[11] Selected actinomycetes were grown in parallel in six different culture media, and the respective metabolomes were compared by TLC analysis and antimicrobial activity assays against *Bacillus subtilis* 168. Among these, *Streptomyces* sp. QL37 grown in static MM yielded the richest metabolic profile, and was therefore subjected to large-scale (7.5 liter) fermentation. Repeated chromatographic separation of TLC-detectable compounds in the resolved crude extract (2.3 g) resulted in **1** (0.5 mg), **2** (27 mg), **8/9** (27 mg), **10** (3.4 mg), and **13** (1 mg).

Lugdunomycin (**1**) was obtained as a colorless amorphous powder. UHPLC-ToF-MS analysis identified $[M + H]^+$ ion peak at *m/z* 474.1553 (calculated for $C_{27}H_{24}NO_7$ 474.1547) that established its molecular composition $C_{27}H_{23}NO_7$. This deduced chemical formula was

corroborated by the attached proton test (APT) that exhibited 27 carbons in total. The APT experiment separated 11 carbons of CH and/or CH_3 downwards from 16 carbons of C and/or CH_2 upwards. Protonated carbons were subsequently assigned by HSQC spectroscopy as two methyl groups (one methoxyl), two methylenes, nine methines (seven of which were aromatic units). Based on chemical shifts, 14 quaternary carbons were classified as two carbonyls (δ_C 182.4, and 182.5), nine olefinic carbons (three are oxygenated $\delta_C > 145$, and six are non-oxygenated $\delta_C < 145$), two sp^3 hybridization saturated atoms (δ_C 47.9, 47.3), and one unique *O*-bearing spiroatom at δ_C 94.8 (see below). The elucidation of three aromatic rings (ring A, B, and D) in **1** were readily assigned by the interpretation of the proton splitting pattern and COSY correlations, and further confirmed by HMBC (Table 1 and Figure S1). ^{1}H NMR spectrum exhibited typical signals attributable to a 1,2,3-trisubstituted phenyl moiety at δ_H 6.92 (brd, J = 7.8 Hz, H-11), 7.22 (t, J = 7.8 Hz, H-12), 6.96 (brd, J = 7.8 Hz, H-13) for ring D. Ring A presented a group of coupling singlets, including two characteristic *meta* benzene singlets at δ_H 6.57 (brs, H-2), 6.95 (brs, H-4) secluded by an olefinic methyl at δ_H 2.46 (brs, H_3-25). Two distinctive aromatic doublets at δ_H 7.39 (d, J = 8.4 Hz, H-5), 6.78 (d, J = 8.4 Hz, H-6) were assigned to ring B. Benzene rings A and B were fused into a naphthalene system by sharing a double bond between C-4a and C-8a, which was unambiguously confirmed by several HMBC correlations, such as H-4/C-8a, H-5/C-8a, H-4/C-5, H-5/C-4, and H-6/C-4a. However, ring D was located outside the ring A/B system because no HMBC correlations were observed. Adjacent to benzene ring D, ring C was identified by the HMBC correlations from the only proton singlet at δ_H 5.62 (s, H-16) to three aromatic carbons of ring D, via δ_C 139.2 (C-10), 158.4 (C-14), and 123.1 (C-15). On the other hand, the correlations of H-16 with saturated quaternary carbons δ_C 59.8 (C-17), and 62.3 (C-21), demonstrated ring C bridging to other non-aromatic rings. Because ring C was proton-deficient (carrying only a single proton), the continued flow of structure elucidation transferred to a hydrogen-enriched fragment (-CH_2-CH(OH)-CH_2-) that was readily resolved by COSY and HMBC. Key HMBC correlations such as H-19/C-17, H-19/C-21, H-18/C-16, H-20/C-17, and H-20/C-21, *etc* (Table 1), unequivocally demonstrated the presence of cyclopentanol ring F, joined to ring C by sharing the bond between C-17 and C-21. Furthermore, H-18 and H-20 showed $^3J_{CH}$ HMBC correlations with two carbonyl groups at δ_C 182.4, and 182.5, respectively, which indicated the presence of another ring fused to two all-carbon quaternary stereocentres[13] C-17 and C-21 besides rings C and F; these two carbonyls had to be cyclized by a nitrogen atom in line with both the molecular formula and the chemical shifts, which was consistent with succinimide ring G. Consequently, rings D/C/F/G constituted a benzaza[4,3,3]propellane motif which is a molecule with unprecedented chemical topology [2,4-dioxo-7,8-(6-methoxyl-benzo)-3-aza[4,3,3]propellan-6,11-diol]. This ring system stereoscopically resembles a propeller: the rings D/C, F, G would be the propeller's blades, and the shared C_{17}–C_{21} bond would be its axis. The aforementioned ring systems A/B and D/C/F/G were linked at spiroatom C-9 (δ_C 94.8), which was established by the key HMBC correlations H-20/C-9, H-11/C-9, and H-6/C-9, although usual long range couplings ($^4J_{CH}$) such as H-5/C-1, and H-6/C-9 were considerably misleading (Table 1 and Figure S1). From this we concluded that an additional five-membered furan ring (ring E) was formed to make a 2*H*-naphtho[1,8-*bc*]furan module [7-methy-2*H*-naphtho[1,8-*bc*]furan-3-ol] to join the whole structure. Due to the rigidity of naphthalene, the system of A/B/E was on the same spatial

plane. Taken together, the benzaza[4,3,3]propellane skeleton is adorned with a spirocyclic 2*H*-naphtho[1,8-*bc*]furan moiety and two all-carbon quaternary centers embedded within five contiguous stereogenic carbons. The striking architecture of benzaza[4,3,3]propellane-6-spiro-2'-2*H*-naphtho[1,8-*bc*]furan has a so far unprecedented chemistry.

Table 1. ^{1}H and ^{13}C NMR data for Lugdunomycin (**1**) [a]

NO.	δ_C	δ_H (*J* in Hz)	HMBC [b]	COSY	NOESY
1	158.8				
2	102.4	6.57 (brs)	C-8a, C-4, C-25	H-4, H-25	H-25
3	136.2				
4	115.7	6.95 (brs)	C-8a, C-2, C-25, C-5	H-2, H-25	H-25
4a	127.4				
5	127.1	7.39 (d, *J* = 8.4 Hz, 1H)	C-4, C-8a, C-7, C-6, C-1*, C-8*	H-6	
6	123.9	6.78 (d, *J* = 8.4 Hz, 1H)	C-4a, C-8, C-7, C-9*	H-5	
7	148.2				
8	122.3				
8a	129.1				
9	94.8				
10	139.2				
11	119.7	6.92 (brd, *J* = 7.8 Hz, 1H)	C-9, C-13, C-15	H-12, H-13	
12	130.9	7.22 (t, *J* = 7.8 Hz, 1H)	C-10, C-14, C-13, C-11	H-11, H-13	
13	111.1	6.96 (brd, *J* = 7.8 Hz, 1H)	C-11, C-15, C-14	H-12, H-11	H-26
14	158.4				
15	123.1				
16	62.6	5.62 (s)	C-15, C-14, C-10, C-17, C-18, C-21		H-18b, H-20a
17	59.8				
18	47.9	2.64 (m, H-18a);	C-24, C-19, C-20, C-16	H-18b	H-18b, H-20b
		1.62 (dd, *J* = 13.8, 3.6 Hz, H-18b)	C-24, C-17, C-16, C-19	H-19, H-18a	H-20a, H-16, H-19, H-18a
19	70.5	4.09 (t, *J* =3.6 Hz, 1H)	C-17, C-18, C-20, C-21	H-18b, H-20b	H-18b, H-20b, H-20a
20	47.3	2.63 (m, H-20a)	C-17, C-19, C-18, C-22	H-20b	H-19, H-18b
		2.40 (dd, *J* = 14.4, 3.6 Hz, H-20b)	C-22, C-9, C-21	H-19, H-20a	H-19, H-18a, H-20a
21	62.3				
22	182.5				
23	-NH				
24	182.4				
25	22.1	2.46 (brs, 3H)	C-2, C-3, C-4	H-2, H-4	H-2, H-4
26	56.1	3.90 (s, 3H)	C-14		H-13

[a] **1** recorded in CD_3OD. Proton coupling constants (*J*) in Hz are given in parentheses. ^{1}H NMR and ^{13}C APT NMR spectra were recorded at 600 MHz. All chemical shift assignments were done on the basis of 1D and 2D NMR techniques. [b] All observed HMBC, COSY, and NOESY correlations are summarized, and long range coupling ($^{4}J_{CH}$) in HMBC was marked with asterisk (*****).

The planar structure was confirmed by single-crystal X-ray diffraction analysis of lugdunomycin (**1**) crystalized from $CHCl_3$/MeOH 10:1 (Table S1), and the absolute configurations of five chiral centers were accordingly determined as 9*R*, 16*R*, 17*R*, 19*R*, 21*S* (Figure 2). Crystallization of **1** in a chiral space group was initially puzzling, as it exhibited a centrosymmetric space group $P\bar{1}$, suggesting presence of a racemic mixture (Figure S2), but enantiomers were not in a 1:1 ratio. In 3D space, an intramolecular hydrogen-bonding interaction between 16-OH (H acceptor) and 7-OH (H donor), further ensured the rigidification of backbone and fixed geometric conformation. To complicate the story more, we encountered two different crystal forms in the crystallization trial. Unfortunately, one crystal form did not diffract well enough to resolve the structure. Judging by the space group,

these two crystals are diastereomers. The Diels-Alder mechanism (see Figure 3) echoed with the observed stereochemistry of lugdunomycin (**1**) in the crystallization trial. Asymmetrical 3-hydroxypathalimide employing either "*endo*" or "*exo*" transition states can lead to adducts of enantiomeric stereochemistry at four carbons, via C-9, C-17, C-19, and C-21 of lugdunomycin. Electron-withdrawing carbonyls are oriented towards the diene π system in the *endo* orientation, while away from it in the *exo* orientation. It is noteworthy that the "*endo*" is typically favored for rigid dienophile, which explained the unbalanced titer of enantiomers in lugdunomycin crystal. The diastereochemistry implied in crystallization experiment could arise from Michael addition step at C-16, because H_2O attacked the double bond from either rear or front face.

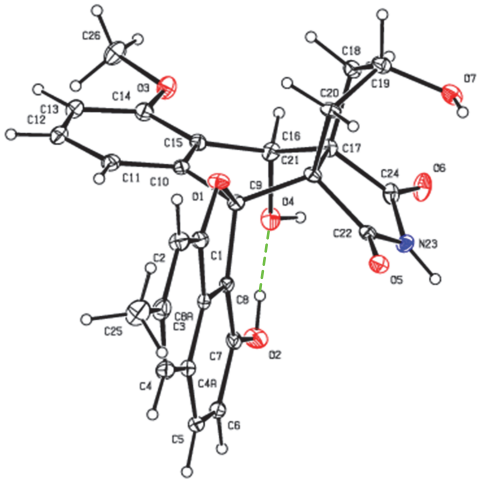

Figure 2. ORTEP drawing of the crystal structure of lugdunomycin (1). The dashed green line represents an intramolecular H-bond between two hydroxyl groups (16-OH and 7-OH). The relative configurations of five chiral centers are 9*R*, 16*R*, 17*R*, 19*R*, 21*S*.

2.2. The biosynthetic pathway of lugdunomycin (1)

Elucidating the biosynthesis pathway of lugdunomycin (**1**) is challenging, because of the high structural complexity of the molecule. It is not uncommon that a single organism simultaneously produces many structurally related analogues. The structures of the lower order intermediates or side products reflect the way the initial precursor is made, which could provide clues to elucidate the bioassembly mechanism of a higher order final product. In this sense, systematic isolation of all compounds, despite being time-consuming and labor-intensive, is not only efficient to bring to light the chemical diversity of the natural products produced by a given producer organism, but also allows dissecting unfamiliar chemical skeletons in terms of structure elucidation (2D planar connection and even 3D absolute configuration) and the biosynthetic pathway. Herein, lugdunomycin (**1**) was proposed to be an angucycline/one derivative, because i) compound **1** was co-isolated with angucycline/ones **2**, **8—10**, and **13**; ii) the structural residue of rings A/B/D in **1** is exactly the same as in **2**. Thereby, **2** was supposed to be the precursor of **1**, but it was difficult to explain the origin of rings C, E—G, especially for the introduction of an unique nitrogen atom into the angucycline/one backbone.

To improve the production of lugdunomycin (**1**) and its structurally related congeners, *Streptomyces* sp. QL37 was fermented in 77 different culture media (Table S2), varied in terms of culturing mode (liquid or solid), source of carbon, phosphate or nitrogen, pH, additional additives, *etcetera*. The EtOAc-resolved metabolome was analyzed by HPLC-UV (detected at 210 nm), which showed that growth on R5 agar plates with 0.8% peptone and 1%

mannitol triggered the production of a considerable number of compounds with a UV spectrum analogous to lugdunomycin (Figure S3). Further UHPLC-ToF-MS analysis confirmed that these compounds indeed contained the sought-after nitrogen atom, though lugdunomycin (**1**) itself was not detected in the mixture. Up-scale refermentation (20 liter) of *Streptomyces* sp. QL37 followed by the extensive systematic isolation, enabled the identification of unrearranged (**2**−**14**) and rearranged (**15**−**31**) angucycline/ones (Figure 1), whereby **5**−**7**, **10**, **11**, **16**−**21**, **24**, **26**−**31** were previously undescribed structures. The structure identification was done on the basis of NMR (1D and/or 2D) and UHPLC-ToF-MS analysis in positive and/or negative modes, which were compared with literature spectroscopic data. The 18 new compounds featured among others unique ring rearrangement/cleavage (**15**−**31**), hydration (**18**−**21**), methanolysis (**16**, **17**, **19**, **20**), epoxidation (**7**), *N*-quaternary methylation (**21**), and amidation (**15**−**24**, and **29**−**31**), which adds further chemical diversity and new members to the family of angucycline antibiotics. Particularly, compounds **5** and **6** possess the rare substituents diazo and nitroso group at C-6, respectively.

The co-identification of compounds **2**—**31** in *Streptomyces* sp. QL37 provided evidences for the biosynthetic route of lugdunomycin (**1**), as proposed in Figure 3. The type II PKS-catalyzed assembly of the angucycline benz[a]anthracene-7,12-dione in itself has been well documented,[9,10] whereas the post-PKS modification of angucycline backbone was central to the biosynthesis of lugdunomycin. A pivotal Baeyer−Villiger oxidation at the C-6a/C-7 bond of C ring initiated the structural rearrangements of precursors **2** and/or **8** into **15**—**31**, whereas the cleavage at C-1/12b bond of A ring generated tricyclic anthraquinone scaffold **29**—**31**. The oxidation product **2a** was susceptible to hydration to afford **2b** that likely serves as the key intermediate for lugdunomycin (**1**), as well as for all the other rearranged angucyclines **15**—**31**. On the one hand, the 7−COOH group in **2b** could be furnished by a putative transaminase, and a subsequent intramolecular cyclization between 7-NH_2 and 12-CO in the resultant amidation product **2d** generated a five-membered 2-pyrrolidone ring. However, it is not impossible that the amidation reaction was conducted at the 12-CO instead of 7−COOH. Another oxidative C-C cleavage at the bond C-12/12a of limamycin[14]-like intermediate **18a** (or other similar rearranged angucyclines such as **22**—**24**) resulted in a free 3-hydroxypathalimide, which could be deduced by the isolation of **27** and **28**. On the other hand, the intermediate **2b** could instead be transformed through intramolecular hemiacetal reaction between 1-OH and 12-CO, followed by an elimination of H_2O and tautomerization to produce an unsaturated aldehyde intermediate **2c**. Convergent coupling of reactive **2c** and 3-hydroxypathalimide dienophile through Diels−Alder [4+2] cycloaddition constructed a complex system of benzaza[4,4,3]propellane in **1a**. Interestingly, this unconventional mechanism is recently used by Melchiorre et al. to synthesize hydroxy-*o*-quinodimethanes.[15] The α,β-unsaturated carbonyl structural unit in **1a** is susceptible to polar protic solvent nucleophiles like H_2O and MeOH, whereby Michael addition could proceed without heating or use of a catalyst.[16] Consequently, lugdunomycin (**1**) was finally synthesized from **1a** through spontaneous domino reactions, involving a sequence of Michael addition of α,β-conjugated enone with nucleophile reagent H_2O, nucleophilic Favorskii rearrangement, and release of one molecule of CO_2. It is noteworthy that the Favorskii-type rearrangement was also seen in the biosynthesis of the antibiotic enterocin, which was catalyzed by a

flavoenzyme EncM.[17]

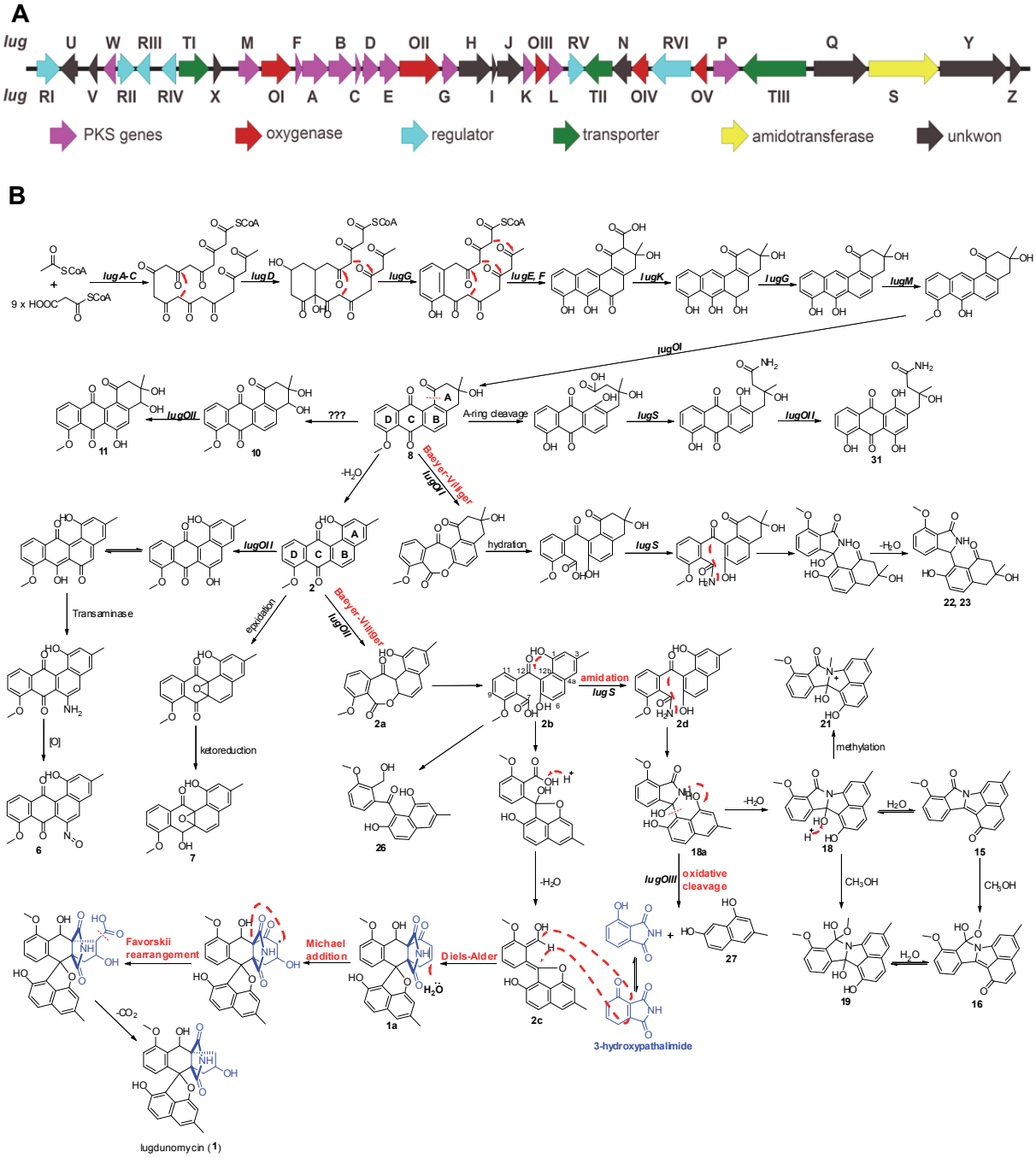

Figure 3. Biosynthetic route to lugdunomycin (1). (A) Organization of the type II PKS gene cluster (*lug*) responsible for lugdunomycin (**1**) biosynthesis in *Streptomyces* sp. QL37. Annotations of respective gene are displayed in Table 2, and genes are depicted in five different colors according to general functions. (B) Expected synthesis route for lugdunomycin and other angucyclines antibiotics presented in Figure 1. All of the compounds in Figure 1 are biosynthetically related. Lugdunomycin likely originates from Baeyer−Villiger oxidative cleavage at the D ring of compound **2,** which is presumably executed by oxygenase *lugOII*. The reactive aldehyde group is thereby non-enzymatically coupled with one molecule of 3-hydroxypathalimde through Diels−Alder [4+2] cycloaddition, followed by spontaneous domino reactions, involving a sequence of Michael addition of α,β-conjugated enone with nucleophile reagent H_2O, nucleophilic Favorskii rearrangement, and release of one molecule of CO_2.

Table 2. Gene organization of the angucycline biosynthetic gene cluster (*lug*) in *Streptomyces* sp. QL37.

ORF	Protein	Distribution	AA	Putative function	Nearest homologue	Homology	Accession
1	LugRI	Prokka_02560	379	XRE-family regulator	*Streptomyces griseoaurantiacus* M045	80%	EGG46652.1
2	LugU	Prokka_02561	284	ADP-ribose pyrophosphatase	*Streptomyces aurantiacus* JA 4570	84%	EPH39897.1
3	LugV	Prokka_02562	144	hypothetical protein	*Streptomyces aureofaciens*	76%	WP_052839114.1
4	LugW	Prokka_02563	199	NADPH-dependent FMN reductase	*Streptomyces sp.* 303MFCol5.2	85%	WP_020127613.1
5	LugRII	Prokka_02564	280	XRE family transcriptional regulator	*Streptomyces sviceus*	81%	WP_007383482.1
6	LugRIII	Prokka_02565	223	LuxR family transcriptional regulator	*Streptomyces sp.* W007	52%	WP_007453015.1
7	LugRIV	Prokka_02566	239	TetR family transcriptional regulator	*Streptomyces sp.* W007	67%	WP_007453018.1
8	LugTI	Prokka_02567	493	putative export protein	*Streptomyces sp.* W007	76%	WP_007453020.1
9	LugX	Prokka_02568	144	hypothetical protein	---	---	---
10	LugM	Prokka_02569	346	*O*-methyltransferase (*tcmO*)	*Streptomyces sp.* W007	71%	WP_007453021.1
11	LugOI	Prokka_02570	490	Monooxygenase (*urdE*)	*Streptomyces sp.* W007	81%	WP_007453024.1
12	LugF	Prokka_02571	109	polyketide cyclase (*urdF*)	*Streptomyces sp.* SCC 2136	80%	CAH10118.1
13	LugA	Prokka_02572	427	polyketide α-ketoacyl synthase II (*urdA*)	*Streptomyces sp.* W007	87%	WP_007453026.1
14	LugB	Prokka_02573	407	polyketide β-ketoacyl synthase (*urdB*)	*Streptomyces sp.* W007	80%	WP_007453027.1
15	LugC	Prokka_02574	91	Acyl carrier protein (*urdC*)	*Streptomyces sp.* W007	71%	WP_007453028.1
16	LugD	Prokka_02575	262	ketoacyl reductase (*urdD*)	*Streptomyces sp.* W007	83%	WP_007453030.1
17	LugE	Prokka_02576	316	aromatase	*Streptomyces sp.* W007	79%	WP_007453031.1
18	LugOII	Prokka_02577	656	monooxygenase (*urdM*)	*Streptomyces sp.* W007	76%	WP_007453032.1
19	LugG	Prokka_02578	262	NAD(P)H dependent dehydrogenase	*Streptomyces sp.* W007	76%	WP_007453033.1
20	LugH	Prokka_02579	527	methylmalonyl-CoA carboxyltransferase	*Streptomyces sp.* W007	87%	WP_007453034.1
21	LugI	Prokka_02580	79	putative acetyl-CoA carboxylase	*Streptomyces rapamycinicus*	61%	WP_020868207.1
22	LugJ	Prokka_02581	417	putative MFS-type transporter EfpA	*Streptomyces sp. 303MFCol5.2*	62%	WP_020130977.1
23	LugK	Prokka_02582	195	NAD(P)H-dependent FMN reductase	*Streptomyces fradiae*	66%	KDS84998.1
24	LugOIII	Prokka_02583	214	putative monooxygenase	*Streptomyces sp.* W007	62%	WP_007450404.1
25	LugL	Prokka_02584	245	phosphopantetheinyl transferase	*Streptomyces venezuelae*	51%	WP_015037371.1
26	LugRV	Prokka_02585	267	transcriptional regulatory protein BaeR	*Streptomyces sp.* W007	66%	WP_007450396.1
27	LugTII	Prokka_02586	458	MFS transporter	*Streptomyces ochraceiscleroticus*	76%	WP_051862838.1
28	LugN	Prokka_02587	307	thioesterase	*Streptomyces scopuliridis*	69%	WP_030349255.1
29	LugOIV	Prokka_02588	275	oxidoreductase	*Streptomyces sp.* W007	70%	WP_050987713.1
30	LugRVI	Prokka_02589	646	SARP family transcriptional regulator	*Streptomyces sp.* W007	57%	WP_007450402.1
31	LugOV	Prokka_02590	229	putative dehydrogenase-methyltransferase	*Streptomyces sp.* W007	57%	WP_007450403.1
32	LugP	Prokka_02591	425	phosphoribosyltransferase	*Streptomyces pratensis*	90%	WP_014156222.1
33	LugTIII	Prokka_02592	1032	secreted protein	*Streptomyces pristinaespiralis* ATCC 25486	81%	EDY62729.1
34	LugQ	Prokka_02593	869	hypothetical protein	*Streptomyces pristinaespiralis*	73%	WP_053557574.1
35	LugS	Prokka_02594	1134	putative Type 1 glutamine amidotransferase	*Streptomyces pristinaespiralis*	75%	WP_005320663.1
36	LugY	Prokka_02595	1093	hypothetical protein	*Streptomyces pristinaespiralis*	78%	WP_005320665.1
37	LugZ	Prokka_02596	185	acetyltransferase	*Streptomyces sp.* W007	72%	WP_032790623.1

Elucidation of the biosynthesis pathway of lugdunomycin (**1**) by the OSMAC strategy shed light on its underlying biosynthetic machinery. Genomic mining of *Streptomyces* sp. QL37 identified a type II polyketide synthase (PKS) gene cluster (*lug*, Table 2 and Figure 3A) displaying a high degree of similarity to PKS gene of *urd*.[18] Genetic inactivation of minimal PKS genes *lugA*–*C* unambiguously confirmed *lug* was responsible for the production of angucycline/ones in *Streptomyces* sp. QL37 (Figure 4). Within the *lug* biosynthetic gene cluster, five genes encoding putative oxygenases, namely *lugOI*–*lugOV*, attracted special attention, since multiple post-PKS oxidations were observed in the isolated angucyclines **1**–**31**, including cleavage of C-C bonds at C-6a/C-7, C-12/12a, and C-1/12b, epoxidation at

C-6a/12a, hydroxylation at C-4 and C-6. The similarity of *lugOI* with *urdE*[19] suggested that this gene is most likely involved in the generation of the *p*-quinone motif to form the basic backbone of angucycline/one. *lugOII* was the best candidate for the C-6a/C-7 Baeyer-Villiger oxygenation, because it shows homologue to *urdM* that is reported to execute this kind of ring oxidative cleavage.[20] To test this assumption, we replaced *lugOII* and *lugOIV* genes with apramycin resistance cassette. HPLC-UV analysis (210 nm) confirmed the biosynthesis of rearranged angucyclines **18**, **22**, and **23,** which requires Baeyer-Villiger ring-opening as requisite, was abrogated in null *lugOII* mutant. Null *lugOIV* mutant gave similar HPLC profiling to wild type, excluding its involvement in the C-6a/C-7 bond cleavage. In addition, gene *lugS* harboring a putative amidotransferase domain was proposed to be responsible for the introduction of nitrogen atom into lugdunomycin (**1**) and rearranged angucyclines **15**–**24**, and **29**–**31**. Subsequent gene knockout of *lugS* confirmed this assumption, since the production of nitrogen-containing angucyclines **18**, **22**, and **23** was abolished in the mutant, while the biosynthetically upstream unrearranged angucyclines **2**, **8**, **9**, and **13** was not affected.

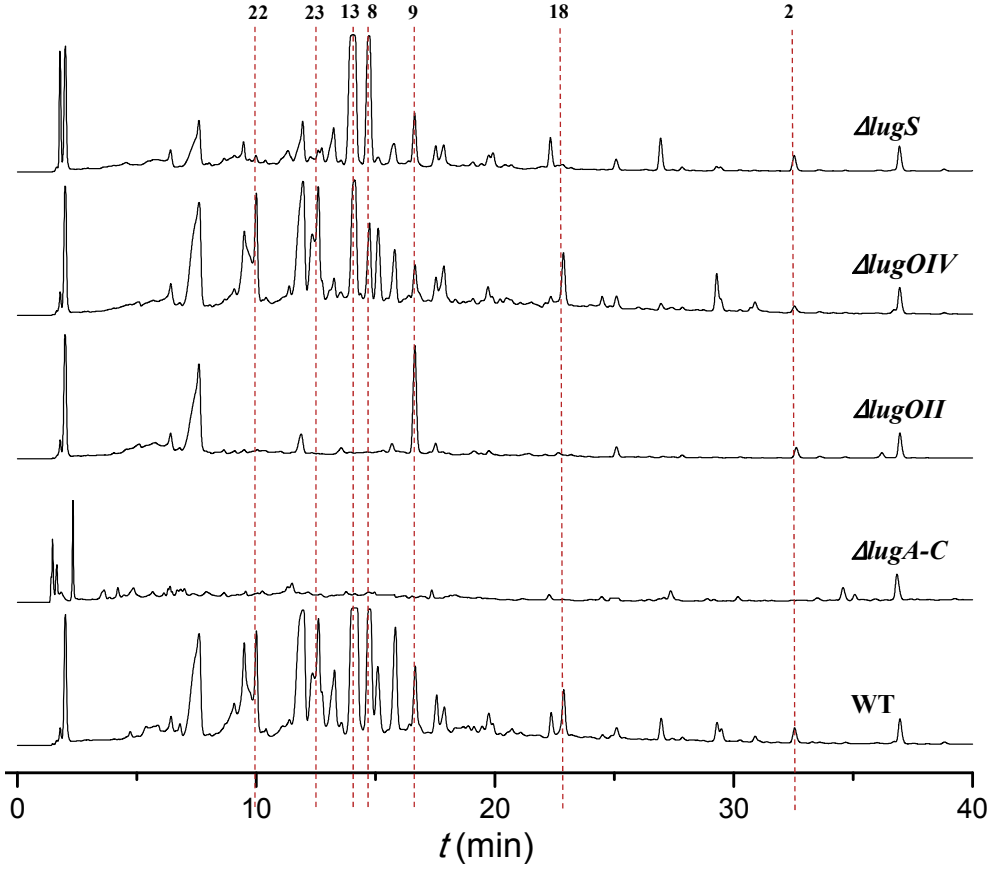

Figure 4. HPLC-UV profiling (210 nm) confirmed functions of selected genes in *lug* cluster. Selected dashed-lined peaks were denoted as compounds with corresponding numbering in Figure 1.

Efforts can be made to improve the supply of two key intermediates for Diels−Alder coupling, via **2b** and 3-hydroxypathalimde. Presumably, *lugOII* could be exploited to increase lugdunomycin production through biochemical transformation (either *in vivo* or *in vitro*) of the abundant precursor **2**. However, it is comparatively more important to overexpress the oxygenase that cleaves the bond C-12/12a, because a considerable amount of limamycins

were already seen in in cultures grown on R5 agar plates with peptone and mannitol, implying that the Baeyer−Villiger cleavage of C-6a/12a was not the rate-limiting step for lugdunomycin (**1**) synthesis. The removal of *lugM* encoding an *O*-methyltransferase probably elevate the production of lugdunomycin variant (26-*O*-demethylated lugdunomycin), because the methyl group blocks the proton tautomerization of 3-hydroxypathalimde into its reactive α,β-unsaturated ketone conformation, and thus hinder the key Diels−Alder reaction for the construction of benzaza[4,4,3]propellane motif in **1a** (Figure 3). Alternatively, the addition of commercial 3-hydroxypathalimde into the culture medium seems more convenient. Taken together, we propose that 1) the biosynthetic route of lugdunomycin, could be used to guide *in situ* optimization of lugdunomycin production in *Streptomyces* sp. QL37. For instance, supplemention of Lewis acid(s) into culture medium to promote Diels−Alder reaction; 2) Lugdunomycin can be constructed through *in vitro* enzymatic Baeyer−Villiger oxidation to generate reactive intermediate, in tandem with semisynthetic method involving Diels−Alder coupling with 3-hydroxypathalimde; 3) By varying the dienophile reagent for Diels−Alder reaction, such as maleimide, *N*-hydroxyphthalimide, maleic anhydride, *etc*, angucycline-based lugdunomycin variants could be potentially synthesized to afford a series of variants of lugdunomycin (Figure S4); 4) The post-PKS modification mode in lugdunomycin biosynthesis, via oxidative quinone ring opening followed by Diels−Alder coupling of extra structural unit at the reactive aldehyde site, can be used to modify other PKS-type natural products, allowing the production of industrially and medicinally important chemicals based on angucyclines, but also other PKS like the linear tetracycline;

2.3. Antimicrobial properties of lugdunomycin (1)

Selected compounds displayed in Figure 1 were tested for antimicrobial activity in an agar diffusion assay, using the Gram-positive *Bacillus subtilis* 168 and the Gram-negative *Escherichia coli* K12 as indicator strains. All tested compounds showed significant antimicrobial activity. Lugdunomycin (**1**) showed antimicrobial activity against *B. subtilis,* but not against *E. coli* (Figure 5). More compound is required to carry out detailed bioactivity assays as well as cytotoxicity and mode of action studies.

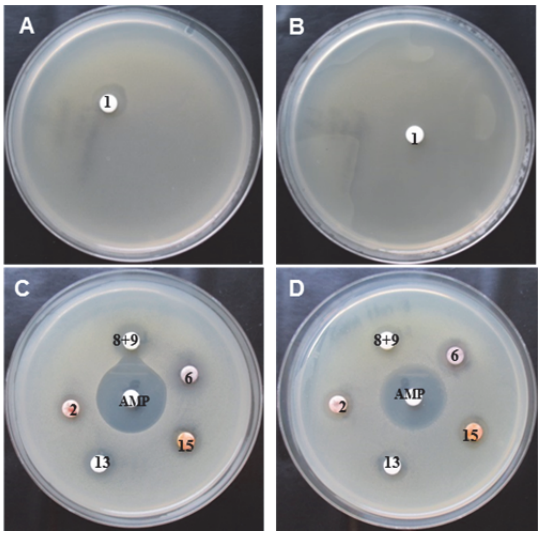

Figure 5. Preliminary antimicrobial activity test of lugdunomycin (1) and selected angucyclines. Numbering on the paper disc corresponds to the numbering of the compounds as presented in Figure 1, e.g. **1** stands for lugdunomycin, **6** for the novel angucycline derivative with nitroso group. Lugdunomycin (**1**) showed inhibition efficacy against Gram-positive bacterium *Bacillus subtilis* (A), but not against Gram-negative *Escherichia coli* JM 109 (B); All the selected angucylines simultaneously inhibited the growth of both *Bacillus subtilis* (C) and *Escherichia coli* JM109 (D). Note: compounds **8** and **9** were obtained as a mixture, which were tested activity together; AMP: postitive control, ampicillin.

3. CONCLUSION

Though synthetic biology approaches tend to dominate the industry of microbial natural products (NPs) discovery,[21] they appear futile in handling intertwined metabolic pathways, such as one biosynthetic gene cluster (BGC) many NPs, many BGCs one NP, and many BGCs many NPs. The OSMAC (one strain many compounds) strategy can complement the genomics-based strain prioritization through direct assessment of all (related) natural products produced under different culturing conditions. Herein, OSMAC applied in *Streptomyces* sp. QL37 allowed the discovery of lugdunomycin (**1**), a novel angucycline-derived molecule harboring a unparalleled backbone of benzaza[4,3,3]propellane-6-spiro-2'-2*H*-naphtho[1,8-*bc*] furan. Tens of co-isolated rearranged and unrearranged angucycline/ones illuminated the "biosynthetic black box" of the unprecedented architectural complexity in lugdunomycin, which also shed light on the characterization of their responsible genetic basis, a type II polyketide synthase gen cluster (*lug*). The genetic and synthetic knowledge revealed in the elucidated biosynthetic pathway for lugdunomycin, especially the Baeyer−Villiger oxidative cleavage and convergent Diels−Alder coupling, is anticipated to not only guide the future up-scale production of lugdunomycin and its potential variants, but also expand the existent structural diversity of known polyketides, which will have profound impact on new drugs development.

4. EXPERIMENTAL SECTION

4.1. General Experimental Procedures

FT-IR was measured on Perkin-Elmer FT-IR Spectrometer Paragon 1000. UV measurements were performed using a Shimadzu UV mini-1240. NMR spectra were recorded on a Bruker DMX 600 MHz, either in methanol-d_4 calibrated to 3.30 ppm or $CDCl_3$ calibrated to 7.27 ppm. Semi-preparative HPLC (pHPLC) was performed with a Shimadzu HPLC system and a 5 ml Rheodyne manual injection loop, equipped with a reversed-phase C_{18} coloumn (Phenomenex Luna C_{18} (2) 100 Å 5 micron 250 × 10 mm). All the pHPLC experiments used 2 ml/min flow rate and fraction collection based on detected peak. Silica gel (pore size 60 Å, 230−400 mesh) for open column chromatography was purchased from Sigma-Aldrich (St. Louis, MO, USA). Pre-coated silica gel 60 F_{254} TLC plates (Merck, Darmstadt, Germany) were used for TLC bioautography analysis. PLC silica gel 60 F_{254}, 1 mm (Merck, Darmstadt, Germany) was used for preparative TLC separation. Analytical TLC was performed with silica gel 60 (Merck, Darmstadt, Germany) plates and visualized with UV lamp (254 nm and 365 nm) and anisaldehyde/sulfuric acid reagent. All solvents and chemicals were of analytical and HPLC grade.

4.2. Microorganisms and culturing conditions

Streptomyces sp. QL37 was isolated from soil in the Qinling mountains (P. R. China) as described previously [11]. The strain was deposited to the collection of the Centraal Bureau voor Schimmelcultures (CBS) in Utrecht, The Netherlands. *Streptomyces* sp. QL37 was cultivated on minimal media agar plates (MM) [22] with 0.5% glycerol and 1% mannitol (w/v) as the carbon sources, and R5 culture medium supplemented with 0.8% peptone and 1% mannitol (w/v). Square agar plates (12 cm × 12 cm) were inoculated with 1 x 10^7 spores from a fresh

spore suspension. As indicator strains for the antibacterial assays we used *Bacillus subtilis* 168 and *Escherichia coli* JM109.

4.3. Extraction and Isolation of lugdunomycin (1)

The first round of systematic separation was done on MM culture medium. After seven days of growth, 225 MM agar plates inoculated with *Streptomyces sp*. QL37 were combined and cut into small blocks, which were then homogenated with a pestle. The resultant agar suspension was extracted with ethyl acetate (EtOAc) by soaking overnight at room temperature. The supernatant was filtered and subsequently evaporated under reduced pressure at 38 °C to obtain 2.3 g crude extract. This extract was adsorbed by silica gel and chromatographed on a silica gel (pore size 60 Å, 70−230 mesh, St. Louis, MO, USA) column chromatography employing a gradient elution from *n*-hexane via chloroform to methanol. The combinations of fractions derived from silica gel chromatography separation were done on the basis of thin-layer chromatography (TLC) analysis (Merck, Darmstadt, Germany) using developing solvent system of chloroform and methanol (10:1). The fractions containing lugdunomycin (**1**) were combined by TLC detection that gave a dark spot under UV at 254 nm and a distinctive blue color when further stained with anisaldehyde/sulfuric acid reagent by heating. Purification of lugdunomycin was first defatted by partition between methanol and *n*-hexane, and the resulting methanol phase was subsequently rechromatographed on Sephadex LH-20 colomn (GE Healthcare Life Sciences, Eindhoven, The Netherlands) eluting by methanol to give five subfractions. The fraction containing lugdunomycin (**1**) was purified by preparative TLC (Merck, Darmstadt, Germany), migrated with solvent system chloroform and methanol (9:1) and detected under UV light at 254 nm. Finally, 0.5 mg pure lugdunomycin (**1**) was obtained. Compounds **2** (3.4 mg), **8/9** (27 mg), **10** (3.4 mg), and **13** (1 mg) were isolated from the same MM agar plates as well.

The second round of separation was done on R5 culture media supplemented with 1% mannitol and 0.8% peptone. A total volume of 20 L R5 agar media was used. The subsequent fermentation and extraction methods were the same with MM culture media. UV and MS-guided separation was used to accumulate the amount of lugdunomycin (**1**) and isolate lugdunomycin analogues. Crude extract (20.5 g) adsorbed by silica gel was first chromatographed on a silica gel column chromatography employing gradient elution from *n*-hexane, chloroform, to methanol, to obtain 17 fractions. These were subsequently subjected to HPLC-UV and UHPLC-ToF-MS analysis, the combination of which was further done by UV spectrum and chemical formula. This identified among others the presence or absence of a nitrogen atom. As a result, 12 final fractions (Fr1−Fr12) were obtained. The fractions (Fr1, Fr4) abundant in already identified compounds **2**, **8−10** in MM medium were discarded. Fr2 was successively chromatographed on silica gel eluting with a gradient of chloroform in *n*-hexane, and Sephadex LH-20 eluting with methanol, to afford pure compound **3** (2.5 mg). Fr3 was separated by silica gel eluting with a gradient of chloroform in *n*-hexane, to give 8 subfractions sfr3.1—sfr3.8. Sfr3.2 was separated by Sephadex LH-20, to afford the pure semi-pure purple compound **6** (0.6 mg); Sfr3.3 was purified by Sephadex LH-20, to afford the pure orange compound **15** (20 mg); Sfr3.5 was firstly separated by Sephadex LH-20 and followed by preparative TLC (PLC Silica gel 60 F_{254}, 1 mm, Merck, Darmstadt, Germany), migrated with solvent system of chlorofomr/methanol (10:1), to afford the semi-pure black

compound **5** (0.6 mg). Fr5 was chromatographed on silica gel eluting with a gradient of methanol in chloroform, to give 5 subfractions sfr5.1−sfr5.5. Sfr5.2 was separated by Sephadex LH-20 to afford pure compound **18** (10 mg); Sfr5.4 was separated by semi-preparative reversed-phase HPLC (Phenomenex Luna C18 (2) 100 Å 5 micron 250 × 10 mm) on an Agilent 1200 series HPLC (Agilent technologies Inc, Santa Clara, CA, USA), eluting with a gradient of ACN in H_2O from 15% to 80% in 40 min. HPLC peaks were manually collected, resulting in the isolation of compound **10** (2.8 mg), **11** (impure, 1.0 mg), **24** (impure, 0.50 mg), **29** (semi-pure, 0.82 mg), **28** (semi-pure, 1.1 mg), **31** (semi-pure, 0.90 mg), and **30** (impure, 0.68 mg). Fr6 was directly separated by semi-preparative HPLC, eluting with a gradient of ACN in H_2O from 15% to 80% in 40 min, which resulted in the separation of compound **14** (semi-pure, 0.80 mg), 7 (semi-pure, 0.40 mg), **25** (semi-pure, 0.30 mg), a mixutre of **27** and **28** (semi-pure, 0.60 mg), and **26** (0.50 mg). Fr7 was directly separated by semi-preparative HPLC, eluting with a gradient of ACN in H_2O from 20% to 85% in 30 min, which resulted in the isolation of **16** (semi-pure, 0.50 mg), **19** (semi-pure, 0.40 mg), and **21** (semi-pure, 0.60 mg). Fr9 was separated by silica gel eluting with a gradient of methanol in chloroform, to give 6 subfractions sfr9.1−sfr9.6. Sfr9.3 was purified by preparative TLC, migrated with solvent system of chlorofomr/methanol (5:1), to afford the pure compound **22** (5 mg) and **23** (5.5 mg).

Lugdunomycin (**1**): colorless, needle crystal, UV (MeOH) λ_{max} (log ε) 349 (3.32), 287 (4.06), 250 (4.42) nm; ECD (MeOH) λ_{max} ($\Delta\varepsilon$) 204 (+4.49), 227 (−4.04), 251 (+0.92) nm; IR ν_{max} 669, 831, 1130, 1203, 1271, 1471, 1558, 1683, 1716, 2324, 2349, 2378, 2850, 2920 cm^{-1}; ^1H and ^{13}C NMR data, see Table 1; HRESIMS (positive mode) *m/z* 456.14481 $[M+H-H_2O]^+$ (calcd for $C_{27}H_{22}NO_6$ 456.14526), 474.15530 $[M+H]^+$ (calcd for $C_{27}H_{24}NO_7$ 474.15473).

4.4. X-ray Crystal Structure Determination of lugdunomycin (1).

Colorless crystals of lugdunomycin (**1**) were obtained from a solvent system of $CHCl_3$/MeOH (10:1). Suitable single crystals for X–ray structural analysis of lugdunomycin were mounted at room temperature in Paratone N inert oil. Single crystal X-ray diffraction data were collected in the home laboratory on a Bruker three circle diffractometer equipped with a Bruker TXS-Mo rotating anode, INCOATEC mirror optics and an APEX II detector. The data were integrated with SAINT and an empirical absorption correction with SADABS [23] was applied. The structure was solved by direct methods.[24] The structure model was refined against all data by full-matrix least-squares methods on F^2 with the program shelxl2014.[25] All non-hydrogen-atoms were refined with anisotropic displacement parameters. The hydrogen atoms were refined isotropically on calculated positions using a riding model with Uiso values constrained to 1.2/1.5 U_{eq} of their parent atoms.

4.5. Antimicrobial activity assays

Antimicrobial activity was determined using a disk diffusion assay. For this, compounds were dissolved in chloroform to a concentration of (2 µg/µl) and of this solution, 25 µl was applied on a paper disk (GE Healthcare Bio-Sciences, Pittsburgh), except for lugdunomycin, for which 10 µl of a 1µg/µl solution in methanol was used. The disks were then placed onto an LB agar plate overlaid with 3 ml of soft agar (LB with 0.6% (w/v) agar) containing around $5x10^7$ cells of exponentially growing *Bacillus subtilis* 168 or *Escherichia coli* JM109 cells.

Ampicillin was used as positive control. After incubation at 37 °C for 18 h, growth inhibition zones (in mm) were recorded as antimicrobial activity.

4.6. Gene knockouts of *lugA—C, lugOII, lugOIV, and lugS*

The methodology for disruption of target genes was based on homologous recombination as illustrated in Figure S5. In general, ~1.5 kb of left and right flanks of target gene were respectively amplified from the *Streptomyces* sp. QL37 genome using the primers listed in Table S3. After digestion with restriction enzymes, the left and right flanks were linked through ~1.0 kb apramycin resistance cassette *aac(3)IV* engineered by enzyme XbaI. The obtaining ~4.0 kb fragment, via left flank─apramycin resistance cassette─right flank, was cloned into the unstable multi-copy vector pWHM3[26] incorporated with *oriT* sequence, to generate the knockout construct. The integrity of the construct was verified by sequencing and restriction enzyme analysis. The correct knockout construct was transformed to the methylase-deficient strain *E. coli* ET12567/pUZ8002, which was further introduced into *Streptomyces* sp. QL37 by conjugation, following the protocol as described.[27] The correct mutant going through double crossover was resistant to 50 μg/mL apramycin and sensitive to 10 μg/mL thiostrepton. The apramycin resistance cassette *aac(3)IV* flanked by loxP sites was removed from the chromosome following the introduction of plasmid pUWLCRE that expresses the Cre recombinase.[28]

4.7. UHPLC-ToF-MS analysis

UHPLC-ToF-MS analyses were performed on an UHPLC system (Ultimate 3000, ThermoScientific, Germany) coupled to an ESI-llQ-TOF spectrometer (micrOTOF-QII, Bruker Daltonics, Germany) in the positive mode. The chromatographic separation was done using a Kinetex C_{18} UHPLC 2.6 μm particle size column 150 × 2.0 mm (Phenomenex, USA) at a flow rate of 0.3 mL/min and a column temperature of 30 ^{o}C. Samples (3 μL) were eluted using a gradient of solvent A (water) and B (acetonitrile), both with 0.1% formic acid (v/v). The initial percentage of B was 5%, which was linearly increased to 90% in 19.5 min, followed by a 2 min isocratic period and, then re-equilibrated with original conditions in 2 min. Nitrogen was used as drying and nebulizing gas. The gas flow was set at 10.0 L/min at 250 ^{o}C and the nebulizer pressure was 2.0 bar. The MS data were acquired over *m/z* range of 100–1000. The capillary voltage was 3.5 kV. For internal calibration, a 10 mM solution of sodium formate (Fluka, Steinheim, Germany) was infused. Formic acid, water and acetonitrile were LCMS grade (Optima, Fisher Scientific, NJ,USA).

4.8. HPLC-UV analysis

HPLC analysis was performed with an Agilent 1200 series HPLC apparatus (Agilent technologies Inc, Santa Clara, CA, USA), using a 150 × 4.6 mm Luna 5 micron C18 (2) 100 Å column equipped with a guard column containing C18 4 × 3 mm cartridges (Phenomenex Inc, Torrance, CA, USA). The mobile phase consisted of water (A) and acetonitrile (B, HPLC grade) in a linear gradient program from 10% B to 100% B in 50 minutes at a flow rate of 1.0 ml/min. Chromatograms were recorded at 210 nm, 254 nm, and 280 nm. The injection volume was 10 μl.

REFERENCES

(1) WHO Geneva, Switserland, 2014.

(2) Payne, D. J.; Gwynn, M. N.; Holmes, D. J.; Pompliano, D. L. *Nat. Rev. Drug Discov.* **2007**, *6*, 29–40.

(3) Raja, A.; LaBonte, J.; Lebbos, J.; Kirkpatrick, P. *Nat. Rev. Drug Discov.* **2003**, *2*, 611–612.

(4) Lewis, K. *Nat. Rev. Drug Discov.* **2013**, *12*, 371–387.

(5) Baltz, R. H. *Curr. Opin. Pharmacol.* **2008**, *8*, 557–563.

(6) Bentley, S. D.; Cerdeño-Tárraga, K. F. C. A.-M.; Challis, G. L.; Thomson, N. R.; James, K. D.; Harris, D. E.; Quail, M. A.; Bentley, S. D.; Harper, D.; Bateman, A.; Brown, S.; Collins, M.; Cronin, A.; Fraser, A.; Goble, A.; Hidalgo, J.; Hornsby, T.; Howarth, S.; Larke, L.; Murphy, L.; Oliver, K.; Rabbinowitsch, E.; Rutherford, K.; Rutter, S.; Seeger, K.; Saunders, D.; Sharp, S.; Squares, R.; Squares, S.; Taylor, K.; Warren, T.; Woodward, J.; Barrell, B. G.; Parkhill, J. *Nature* **2002**, *3*, 141–147.

(7) Zarins-Tutt, J. S.; Barberi, T. T.; Gao, H.; Mearns-Spragg, A.; Zhang, L.; Newman, D. J.; Goss, R. J. M. *Nat. Prod. Rep.* **2016**, *33*, 54–72.

(8) Cooper, M. A.; Shlaes, D. *Nature* **2011**, *472*, 32.

(9) Rohr, J.; Thiericke, R. *Nat. Prod. Rep.* **1992**, *9*, 103–37.

(10) Kharel, M. K.; Pahari, P.; Shepherd, M. D.; Tibrewal, N.; Nybo, S. E.; Shaaban, K. a; Rohr, J. *Nat. Prod. Rep.* **2012**, *29*, 264–325.

(11) Zhu, H.; Swierstra, J.; Wu, C.; Girard, G.; Choi, Y. H.; van Wamel, W.; Sandiford, S. K.; van Wezel, G. P. *Microbiology* **2014**, *160*, 1714–1725.

(12) Brady, S. F.; Chao, C. J.; Handelsman, J.; Clardy, J. *Org. Lett.* **2001**, *3*, 1981–1984.

(13) Minko, Y.; Pasco, M.; Lercher, L.; Botoshansky, M.; Marek, I. *Nature* **2012**, *490*, 522–6.

(14) Fotso, S.; Mahmud, T.; Zabriskie, T. M.; Santosa, D. A.; Proteau, P. J. *J. Antibiot. (Tokyo).* **2008**, *61*, 449–456.

(15) Dell'amico, L.; Vega-Peñaloza, A.; Cuadros, S.; Melchiorre, P. *Angew. Chemie - Int. Ed.* **2016**, *55*, 3313–3317.

(16) Cao, C. M.; Zhang, H.; Gallagher, R. J.; Timmermann, B. N. *J. Nat. Prod.* **2013**, *76*, 2040–2046.

(17) Teufel, R.; Miyanaga, A.; Michaudel, Q.; Stull, F.; Louie, G.; Noel, J. P.; Baran, P. S.; Palfey, B.; Moore, B. S. *Nature* **2013**, *503*, 552–556.

(18) Faust, B.; Hoffmeister, D.; Weitnauer, G.; Westrich, L.; Haag, S.; Schneider, P.; Decker, H.; Künzel, E.; Rohr, J.; Bechthold, A. *Microbiology* **2000**, *146*, 147–154.

(19) Decker, H.; Haag, S. *J. Bacteriol.* **1995**, *177*, 6126–6136.

(20) Rix, U.; Remsing, L. L.; Hoffmeister, D.; Bechthold, A.; Rohr, J. *ChemBioChem* **2003**, *4*, 109–111.

(21) Smanski, M. J.; Zhou, H.; Claesen, J.; Shen, B.; Fischbach, M. A.; Voigt, C. A. *Nat. Rev. Microbiol.* **2016**, *14*, 135–149.

(22) Kieser, T., Bibb, M. J., Buttner, M. J., Chater, K. F. & Hopwood, D. A. John Innes Foundation, Norwich, UK, 2000.

(23) George M. Sheldrick *SADABS, Program for Empirical Absorption Correction of Area*

Detector Data; University of Göttingen: Göttingen, Germany, 1996; Vol. 218.
(24) Schneider, T. R.; Sheldrick, G. M. *Acta Crystallogr. Sect. D Biol. Crystallogr.* **2002**, *58*, 1772–1779.
(25) Sheldrick, G. M. *Acta Crystallogr. A*. **2008**, *64*, 112–122.
(26) Vara, J.; Lewandowska-Skarbek, M.; Wang, Y. G.; Donadio, S.; Hutchinson, C. R. *J. Bacteriol.* **1989**, *171*, 5872–5881.
(27) Kieser T, Bibb M, Buttner M, Chater K, H. D. *Practical Streptomyces Genetics*; John Innes Foundation: Norwich, United Kingdom, 2000.
(28) Fedoryshyn, M.; Welle, E.; Bechthold, A.; Luzhetskyy, A. *Appl. Microbiol. Biotechnol.* **2008**, *78*, 1065–1070.